Electronic Supporting Information

A Novel Nonheme Manganese (II) Complex for (Electro) Catalytic Oxidation of Water†

Dattaprasad N. Narulkar,[a] Koteshwar Devulapally,[b,c] Anil Kumar U.,[d] Sunder N. Dhuri,[*a] Vishal M. Dhavale,[*b,c,d] Anil Kumar Vardhaman,[*b] Lingamallu Giribabu[*b,c]

[a]School of Chemical Sciences, Goa University, Goa-403206, India.

[b]Polymers & Functional Materials Division, CSIR-Indian Institute of Chemical Technology, Uppal Road, Tarnaka, Hyderabad-500 007, India.

[c]Academy of Scientific and Innovative Research (AcSIR), Ghaziabad- 201002, India.

[d]CSIR-Central Electrochemical Research Institute, CSIR Madras Complex, Taramani, Chennai-600 113, India.

E-mail: anil1hnk@gmail.com; vishal.mdhavale@gmail.com; giribabu@iict.res.in; sndhuri@unigoa.ac.in

Materials and methods:

All the chemicals used in this study were purchased from commercial sources. The solvents were dried and distilled prior to use under the N_2 atmosphere. The infrared (IR) spectra were recorded using Shimadzu (IR Prestige-21) FT-IR spectrometer in the region of 4000-400 cm^{-1} by diluting the compounds in KBr powder. The ^{1}H-and ^{13}C-NMR spectra were recorded in $CDCl_3$ on Bruker Avance III 400 MHz NMR spectrometer. The UV-vis spectra were recorded in CH_3CN in the range 200-1000 nm using Agilent diode array 8453 UV-vis spectrophotometer. The EPR spectra were recorded on JEOL JES-FA200 ESR Spectrometer. X-ray photoelectron spectroscopy (XPS) measurements were carried out on a Kratos Analytical, A Shimadzu Group Company Axis Supra^{TM}, at a vacuum pressure of 10^{-9} Torr (pass energy is 20 eV and 160 eV for elemental scan (short) and wide scan (large), respectively. The overall resolution ~0.1 eV.

Electrochemical study:

The electrochemical study was recorded by using Electrochemical Workstation-CH Instrument, Inc. CHI6107. A glass vessel containing sample solution was equipped with three-electrodes namely a glassy carbon electrode (GCE) working electrode, platinum wire as a counter electrode and Ag/AgCl as a reference electrode. The experiments were carried in phosphate buffer solution electrolyte of different pH i.e. 5.2, 7, and 8. Solutions were purged with N_2 gas for around ~30 min prior to the each measurement. Potential (vs. Ag/Ag^{+}) is converted to RHE by using following equation.

$$E_{RHE} = E_{exp}+0.197+0.0591pH$$

Calculation of Faradaic Efficiency (FE) using Rotating Ring Disk Electrode study (RRDE):

RRDE study was carried by using an electrochemical workstation-WaveDriver-200, WaveVertex-10 electrode rotator, Pine Research Instruments.

2 mg of Complex **1** and 2 mg of Vulcan XC-72 carbon is dispersed in 980 μL of DI water. 20 μL of 0.01 wt. % Nafion ionomer is added into the above solution and sonicated in Branson Bath Sonicator for 30 min. The 10 μL of the well dispersed catalyst slurry is used for the drop coating on the disc of RRDE (Pine Research Instruments, E6R2, Disk OD = 5.5 mm; Ring OD = 8.50 mm; Ring ID = 6.50 mm) and dried, and used as a working electrode.

The faradaic efficiency (FE) of Complex **1** for water oxidation reaction was measured by applying a constant current of 1, 5, 10 mA/cm^2 to the modified glassy carbon disk electrode with complex **1** and recorded the ring current. Working electrode was kept at constant 1600 rpm. The constant applied ring potential is 1.3 V.

The collection efficiency (N) of the RRDE electrode was calculated by using ferrocene redox couple and is found to be 0.37.

The Faradaic efficiency is calculated using the equation,

Faradaic efficiency (FE) = $2*I_r/ I_d*N$

where, I_r is the ring current, I_d is 2.374 mA, is the constant disk current for a 0.2374 cm^2 disk electrode to get minimum current density of 10 mA/cm^2 and N is the collection efficiency.

Calculation of TOF:

TOF = j*A / 4nF

where, $j_{\eta=400mV}$ is the current density (A/cm^2), A is the surface area of electrode (cm^2), n is the number of moles of active catalyst, and F is the Faraday constant (C/mol)

Gas chromatography analysis:

Gas chromatographic analysis was performed with a Varian gas chromatograph (Model: cp3800) equipped with a TCD detector using a Carboxen1000 column. Helium was used as the carrier gas. Before the start of experiments, the electrolyte was purged with nitrogen for 20 min. For the oxygen evolution study, we have applied close to onset potential and gas chromatographs were recorded in-situ. A small pipe was placed in the headspace of the home-made cell and directly connected to the GC instrument for the in-situ measurement of

the evolved gas. Here, we have presented the screen shots of GC-spectrum, because of system and software problem. We are unable to get the data points.

Single crystal study:

The single crystals of complex **1** suitable for X-ray studies were picked up and mounted directly on a Bruker SMART APEX-II CCD diffractometer equipped with Mo-K_α = 0.71073Å radiation. The CCD data were integrated and scaled using Bruker-SAINT software package while SHEXTL V 6.12 was used for solving and refining the structures.[46] All non-hydrogen atoms were refined anisotropically, if not stated otherwise. The hydrogen atoms were located at calculated positions.

Synthesis of N3Py2:

Synthesis of *N*,*N′*-dimethyl-*N*-(2-(methyl(pyridin-2-ylmethyl)amino)ethyl)-*N′*-(pyridin-2-ylmethyl)ethane-1,2-diamine)

N3Py2 was prepared by following three step procedures as previously reported in the literature.[1] *Step-I:* To the ethanolic solution of 2-pyridine-carboxaldehyde (3.0 g, 28.0 mmol) was added 1.52 mL of diethylenetriamine (1.44 g, 14.0 mmol). The mixture was refluxed for ~ 5 h, cooled to room temperature and the solvent was removed to give red semisolid product. Yield of product was 3.1 g (79 %). IR data (KBr, cm^{-1}): 3295 ν(N-H), 3200-2700 ν(C-H), 1648 ν(C=N). *Step-II*: To the ice-cold methanolic solution of imine product (3.0 g, 10.7 mmol), the sodium borohydride (0.48 g, 12.8 mmol) was added slowly and the mixture stirred for it became brownish orange in colour (~6 h). The solvent was removed and water (20 mL) was added to the flask containing the crude product. The yellow viscous oil was then extracted using ethyl acetate (30 mL x 3). Yield of product was 2.8 g (92 %). IR data (KBr, cm^{-1}): 3295 ν(N-H), 3200-2700 ν(C-H), 1670 ν(C=N). *Step-III*: The product (2.6 g, 9.1 mmol) of second step was taken in water (3.0 mL) and cooled in ice-bath. To this mixture, formaldehyde (37 %, 22.0 mL) and formic acid (85 %, 15.0 mL) were added and refluxed for

~24 h. The mixture was then cooled and basified (pH = 12) using 2 M NaOH solution. The crude reddish-brown oil obtained after extraction with chloroform (20 mL x 4) was dissolved in HCl solution (pH = ~1). The acidic mixture was then basified using NaOH solution (pH = 12) and the product was then extracted using diethyl ether (20 mL x 6). N3Py2 was formed as yellow oil with the yield 2.5 g (72 %). IR data (KBr, cm^{-1}): 3200-2700 υ(C-H), 1670 υ(C=N).^{1}H NMR ($CDCl_3$, ppm): δ 8.47 (d, 2H, *J* = 3.2 Hz, 2-PyH), δ 7.57 (t, 2H, *J* = 8.2 Hz, 4-PyH), δ 7.34 (d, 2H, *J* =3.8 Hz, 5-PyH), δ 7.08 (t, 2H, *J* = 6.16 Hz, 3-PyH), δ 3.63 (s, 4H, Ar-CH2), δ 2.57 (s, 8H, NCH2), δ 2.25 (s, 3H, NMe), δ 2.25 (s, 3H, NMe) δ 2.21 (s, 6H, NMe). ^{13}C NMR (CDCl3, ppm): δ 159.1 (C6), 148.1 (C2), 136.2 (C4), 122.9(C5), 121.7(C3), 64.04 (Ar-CH_2), 55.3 (NCH_2), 42.7 (N-CH_3).

Synthesis of [Mn(N3Py2)(H_2O)](ClO_4)$_2$] (1)

Ligand N_3Py_2 (0.452g, 1.381 mmol) is dissolved in acetonitrile (2 mL) and added in drops to the constantly stirring acetonitrile solution (2 mL) of $Mn(ClO_4)_2.6H_2O$ (0.5g, 1.381 mmol) under the N_2 atmosphere at room temperature. The mixture was allowed to stir for 12 h to obtain a brownish colored solution. The addition of diethyl ether to this solution gave a white powder which was separated by filtration, washed with diethyl ether and then dried in vacuum. Yield 0.68 g, 82 % Calc. for $C_{19}H_{31}N_5Cl_2O_9Mn$: C, 38.08; H, 4.91; N, 11.69 %. Found C, 38.19; H, 4.91; N, 11.59%. IR (KBr, cm^{-1}): 3412 cm^{-1} ν(O-H); 1093, 621 ν(ClO_4^{-1}).

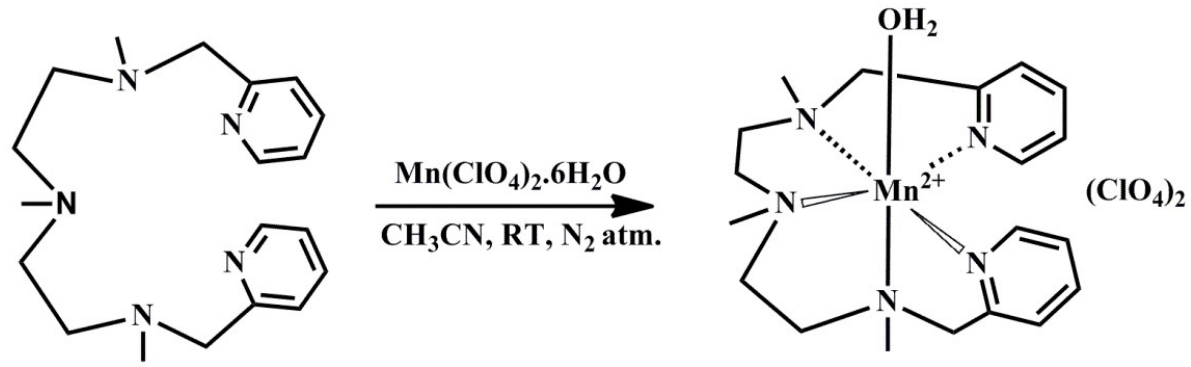

Scheme S1: Synthetic scheme of Complex **1**.

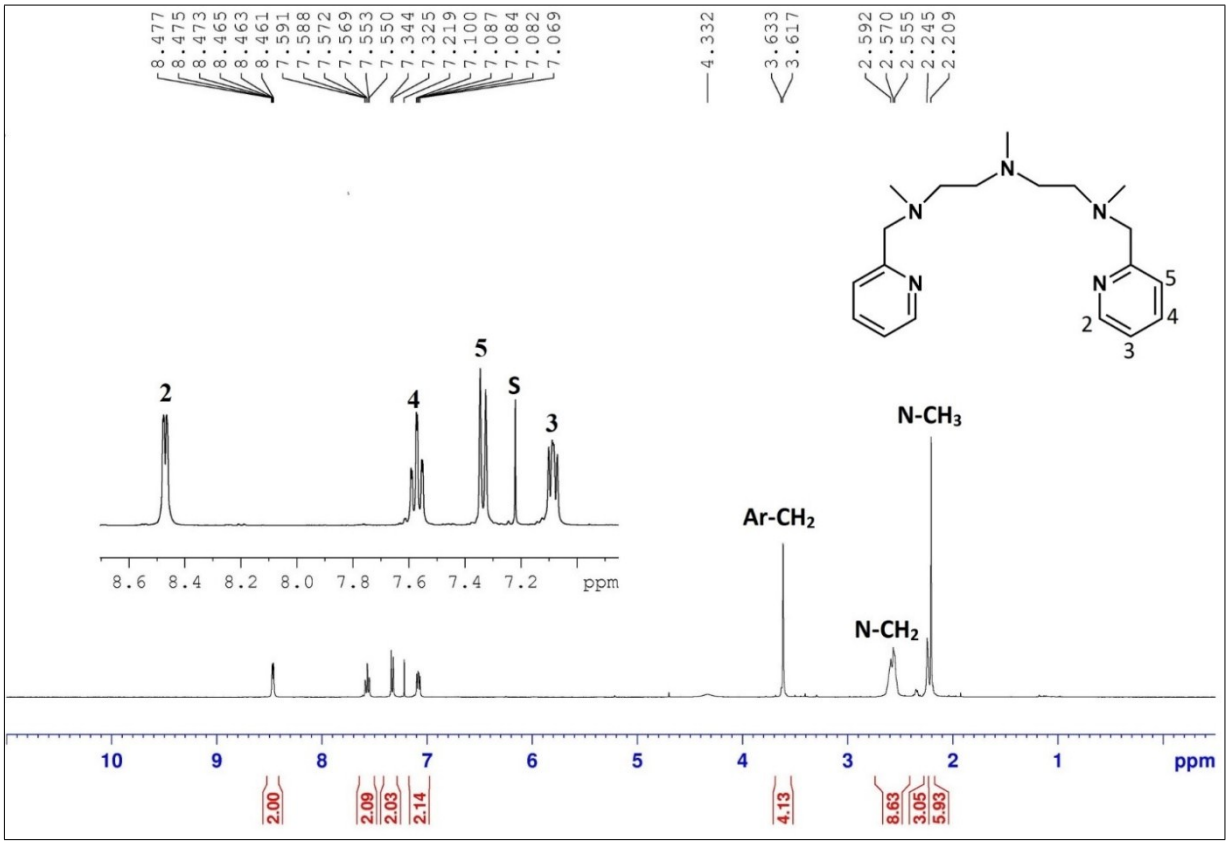

Figure S1: ^{1}H-NMR spectrum of N3Py2 recorded in $CDCl_3$

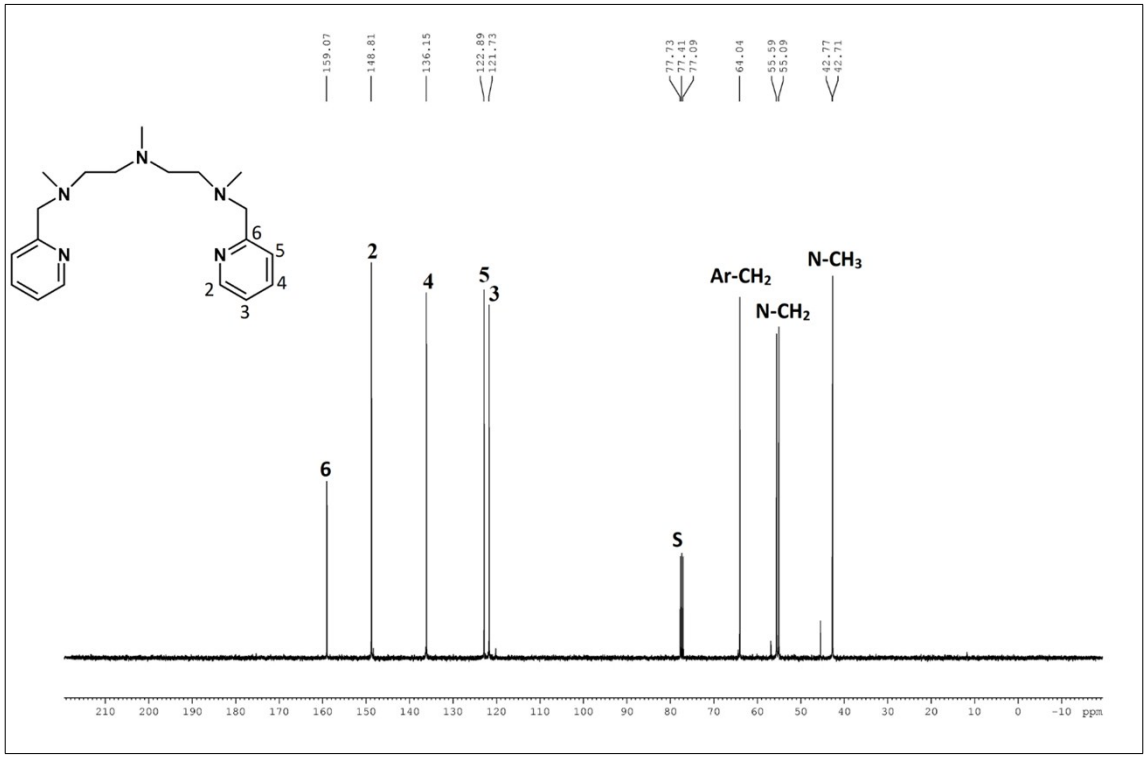

Figure S2: ^{13}C-NMR spectrum of N3Py2 recorded in $CDCl_3$

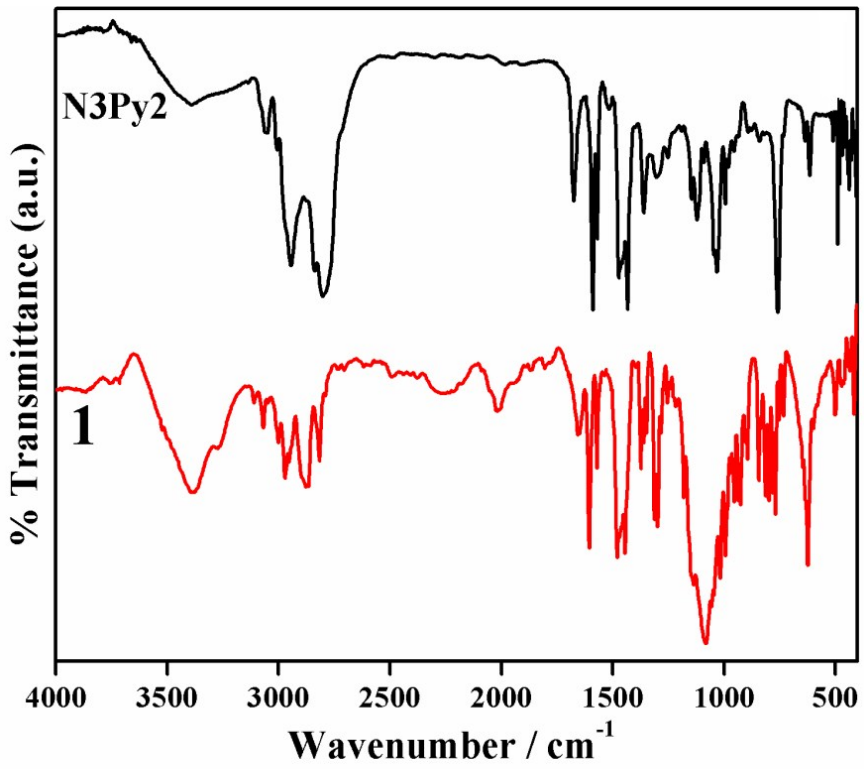

Figure S3: Comparative Infrared spectra of **L** (black trace) and **1** (red trace). IR spectrum of **1** show a band at 3412 cm^{-1} assignable to the O-H vibration of water and while the strong bands at 1091 and 615 cm^{-1} due to charge balancing perchlorates.

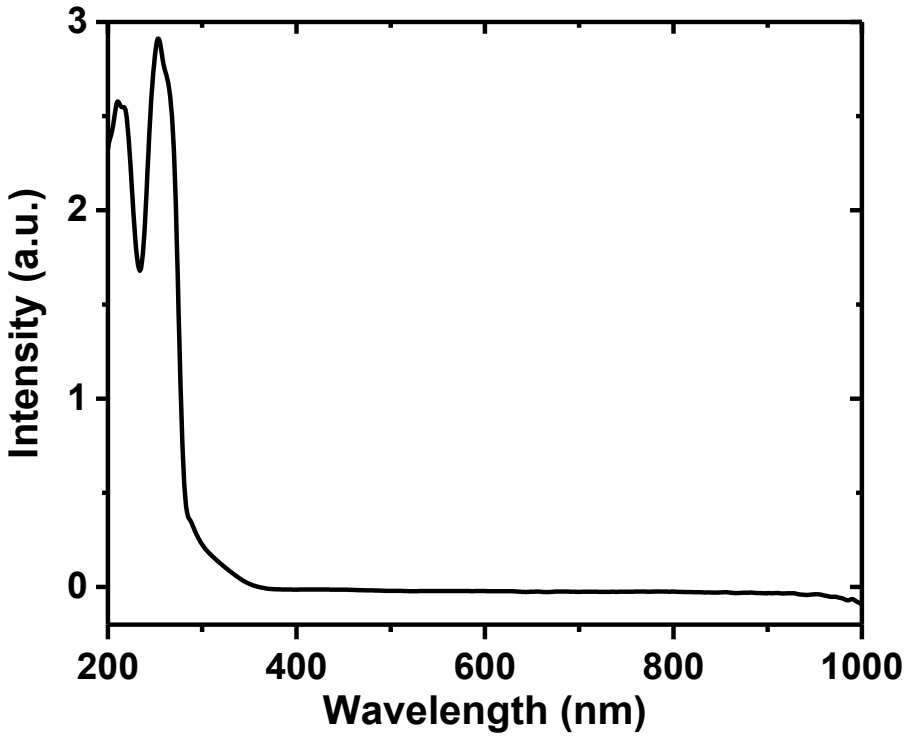

Figure S4: UV-Vis. of Complex **1** recorded in CH_3CN.

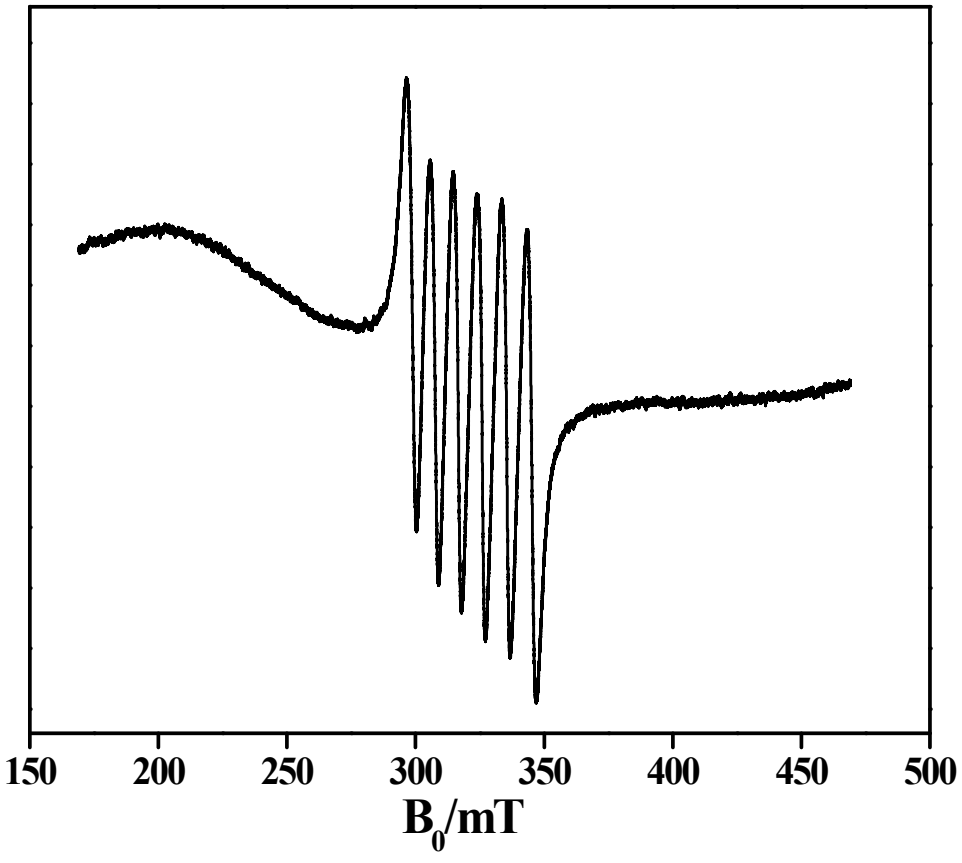

Figure S5: EPR of Complex **1**.

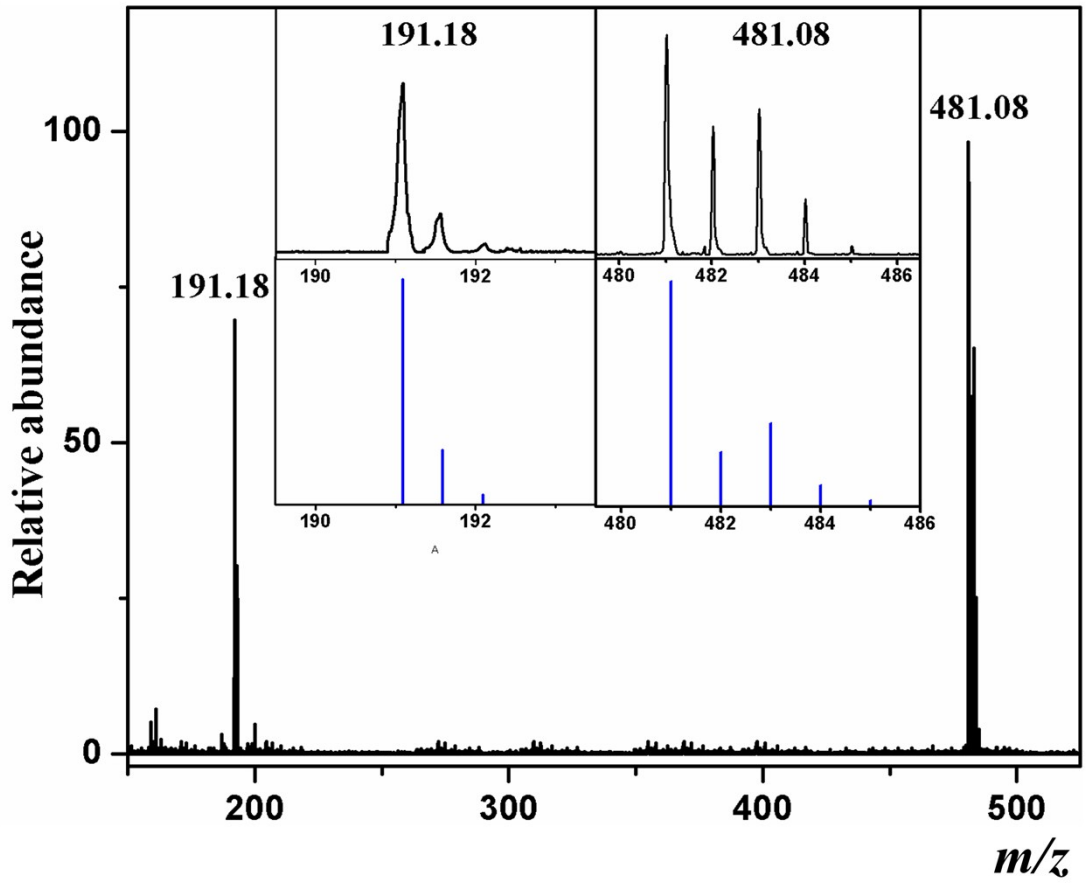

Figure S6: ESI-MS of $[Mn(N3Py2)(H_2O)](ClO_4)_2$ (**1**) recorded in CH_3CN showing a mass peak m/z = 191.18 due to the $[Mn(N3Py2)]^{2+}$ species and peak at m/z = 481.08 due to $[Mn(N3Py2)(ClO_4)]^{+}$ species. The inset shows the isotope distribution patterns for the prominent peaks in black with simulated peaks in blue color.

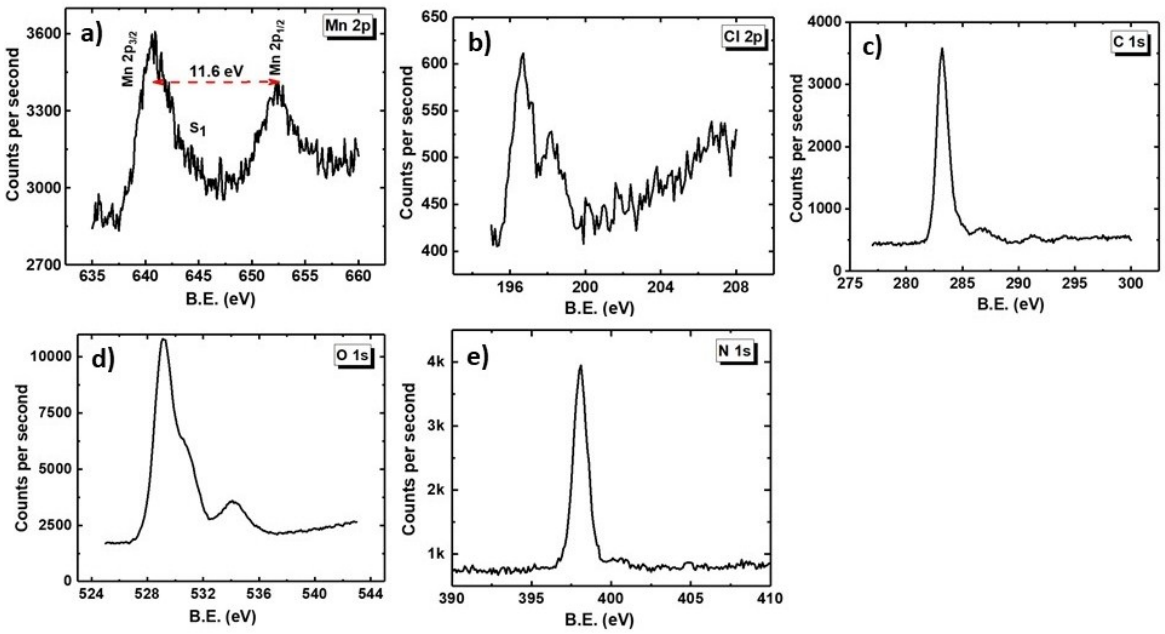

Figure S7: XPS of (a) Mn2p, (b) Cl2p, (c) C1s, (d) O1s, and (e) N1s of Complex **1** before electrochemical water oxidation (BEcWO).

It is clearly indicating the presence of Mn, Cl, C, O, and N and the respective XPS of the elements are presented in **Figure S7a-7e**, respectively. Mn 2p spectrum (**Figure S7a**) displayed the spin-orbit splitting *j* values as 3/2 and 1/2 with specific binding energy difference of 11.6 eV, which support to the oxidation state of Mn present in complex **1** i.e. +2.

The well resolved Mn 2p peaks and absence of satellite peak clearly indicates the compound is pure and no-oxide formation in the Complex **1** (**Figure S7**). However, the satellite peak appeared (at ~646 eV) in Mn 2p spectrum of Complex **1** may be hinting towards binding of Mn-center with oxygen, after electrochemical water oxidation (**AEcWO**) (**Figure S17**), which might be due to the formation of adduct. But it is possible to distinguish Mn-oxides using Mn3s peak,[2] and in present case, we did not observe clear peak for the same. Further investigation is underway.

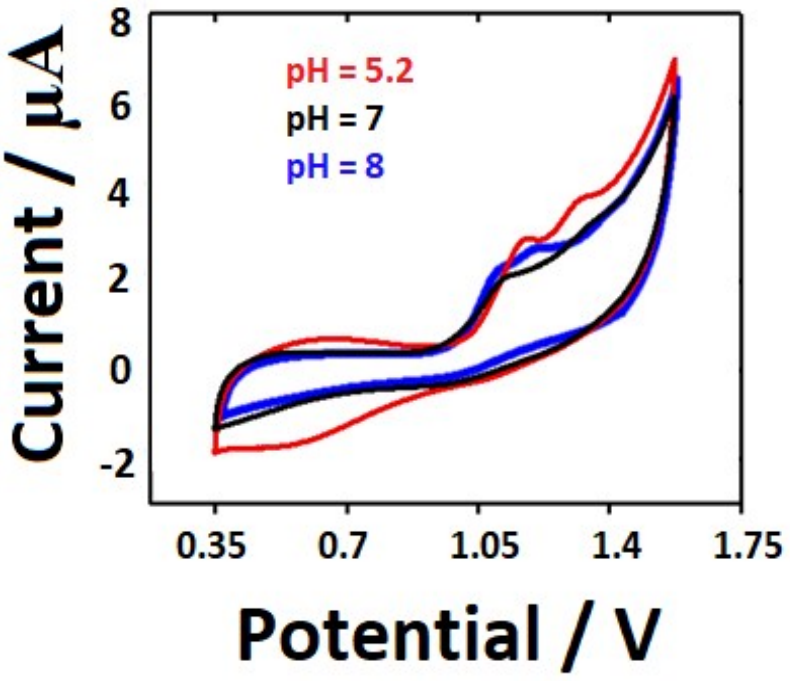

Figure S8: Comparative CVs of Complex **1** recorded in different pH. (Electrolyte: Nitrogen saturated phosphate buffer solution; Scan rate: 100 mV/s).

The cyclic voltammogram of complex **1** obtained in phosphate buffer solutions the irreversible peak in potential range of 1.0 – 1.5 V, might be attributed to the oxidation of Mn^{II} ion to higher oxidation states. The sharp onset of current after a second broader peak (after 1.1 V), is characteristic of water oxidation.

[Generally, it is known in the literature and considered that, the higher oxidation state species are highly reactive and are also very difficult to be trapped.[3]]

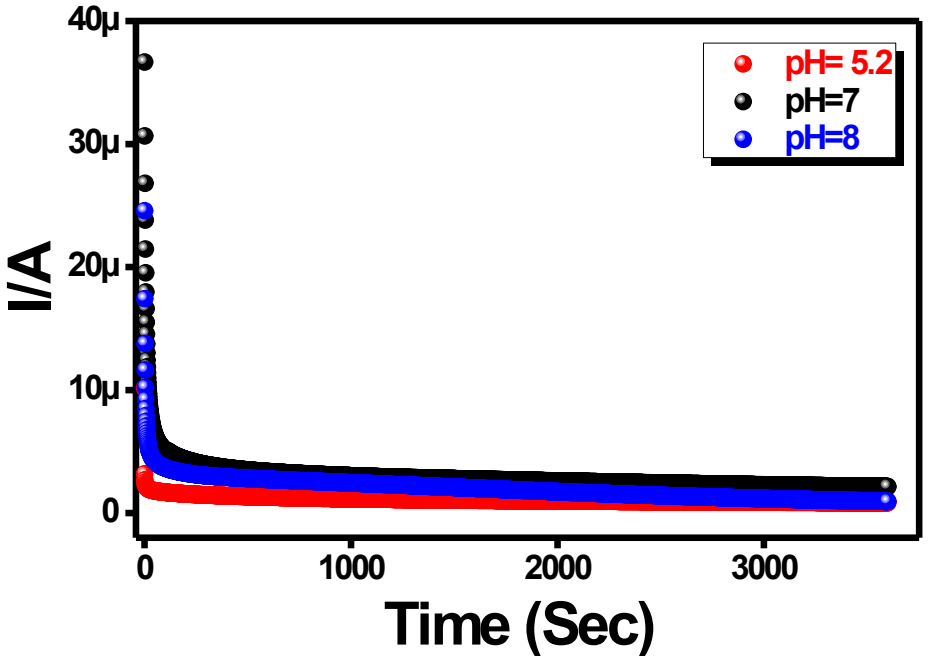

Figure S9: Chronoamperometry stability test of Complex **1** recorded in pH of 5.2 (applied potential is 1.8 V), 7 (applied potential is 1.68 V), and 8 (applied potential is 1.58 V). Electrolyte: Nitrogen saturated phosphate buffer solution.

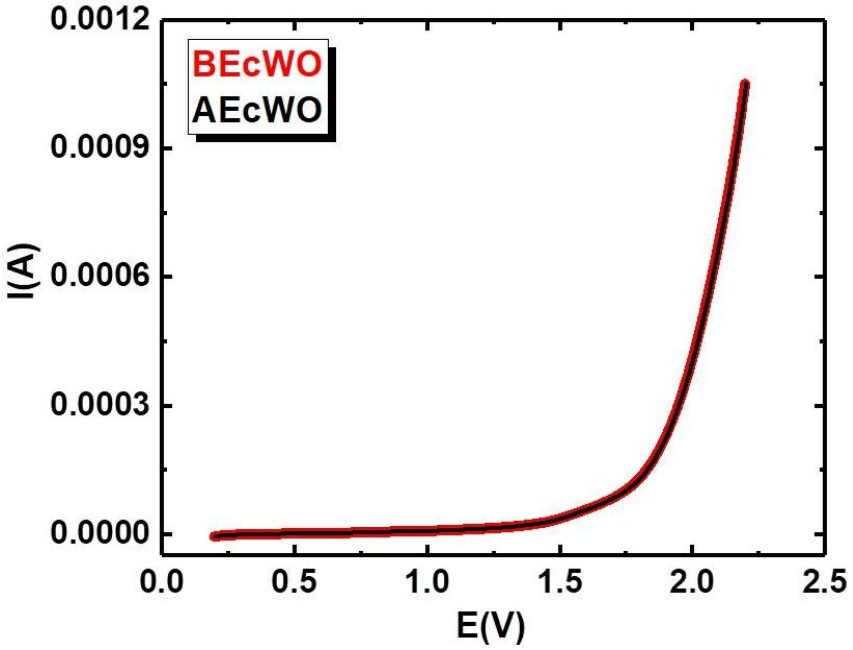

Figure S10: Comparative LSVs of Complex **1** recorded before (BEcWO) and after (AEcWO) the electrochemical oxidation study i.e. Chronoamperometry stability in pH of 5.2. Electrolyte: Phosphate buffer solution; Rotation: 1600 rpm; Scan rate: 50 mV/s.

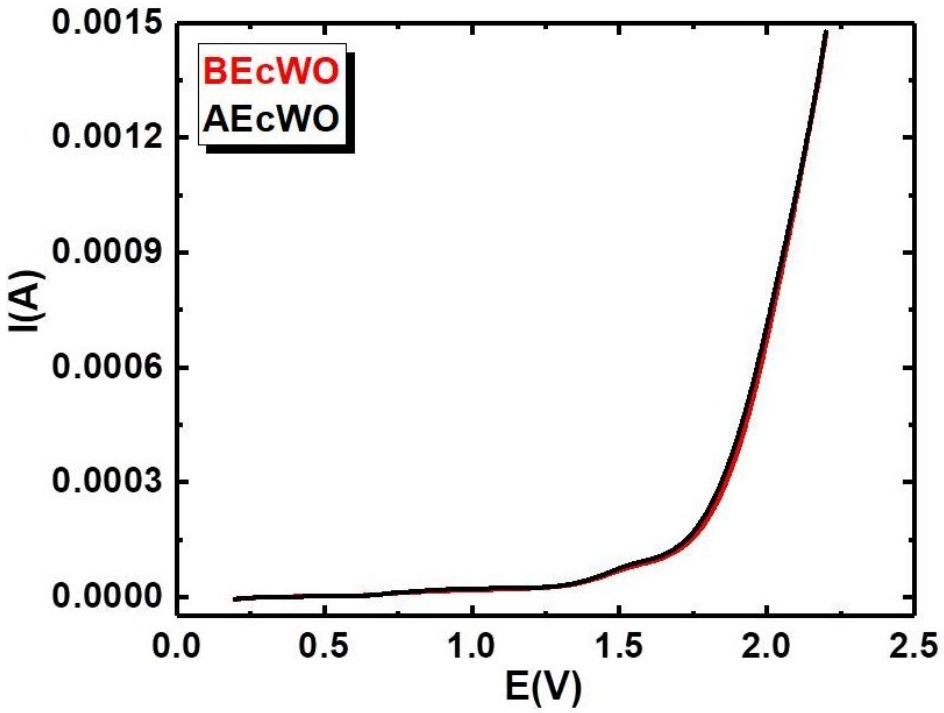

Figure S11: Comparative LSVs of Complex **1** recorded before (BEcWO) and after (AEcWO) the electrochemical oxidation study i.e. Chronoamperometry stability in pH of 7. Electrolyte: Phosphate buffer solution; Rotation: 1600 rpm; Scan rate: 50 mV/s.

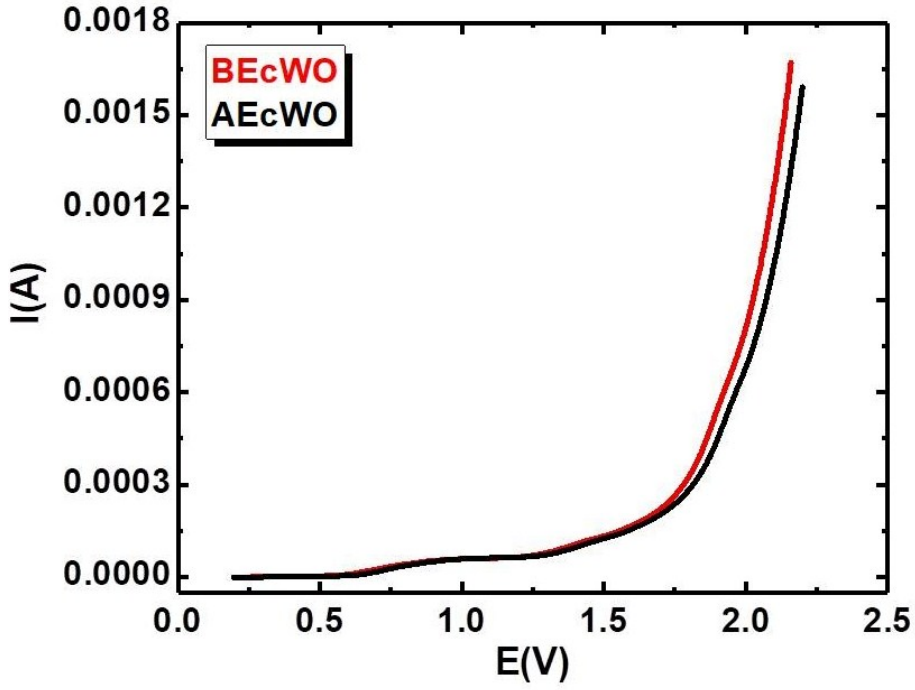

Figure S12: Comparative LSVs of Complex **1** recorded before (BEcWO) and after (AEcWO) the electrochemical oxidation study i.e. Chronoamperometry stability in pH of 8. Electrolyte: Phosphate buffer solution; Rotation: 1600 rpm; Scan rate: 50 mV/s.

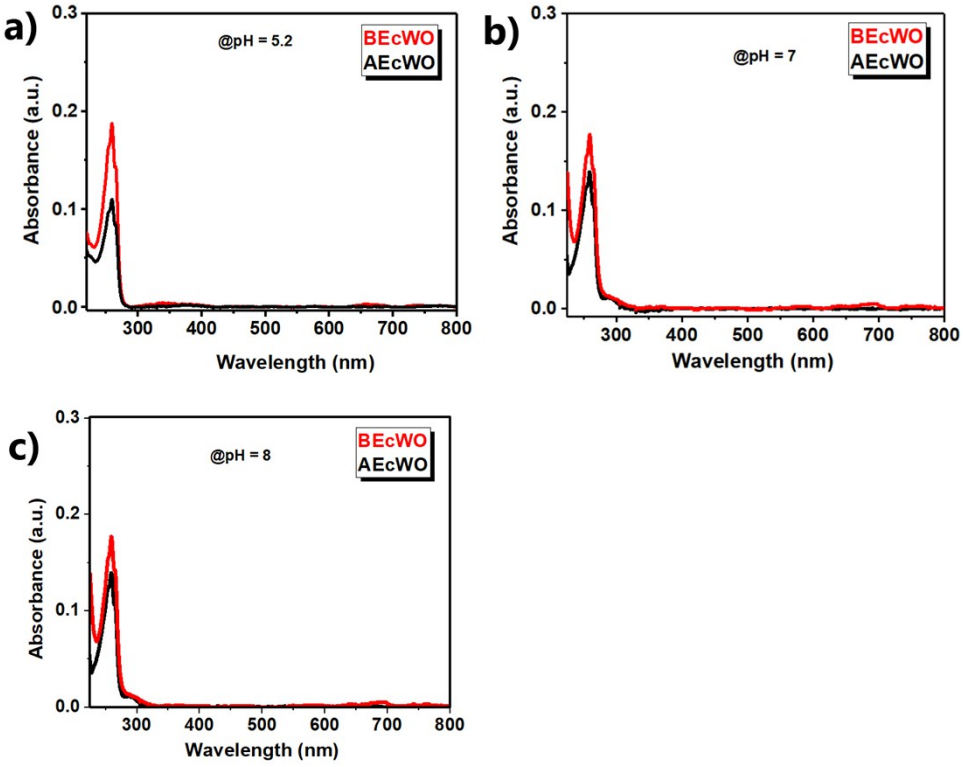

Figure S13: Comparative UV-Vis spectrum of Complex **1** recorded before (BEcWO) and after (AEcWO) the electrochemical water oxidation study i.e. Chronoamperometry stability.

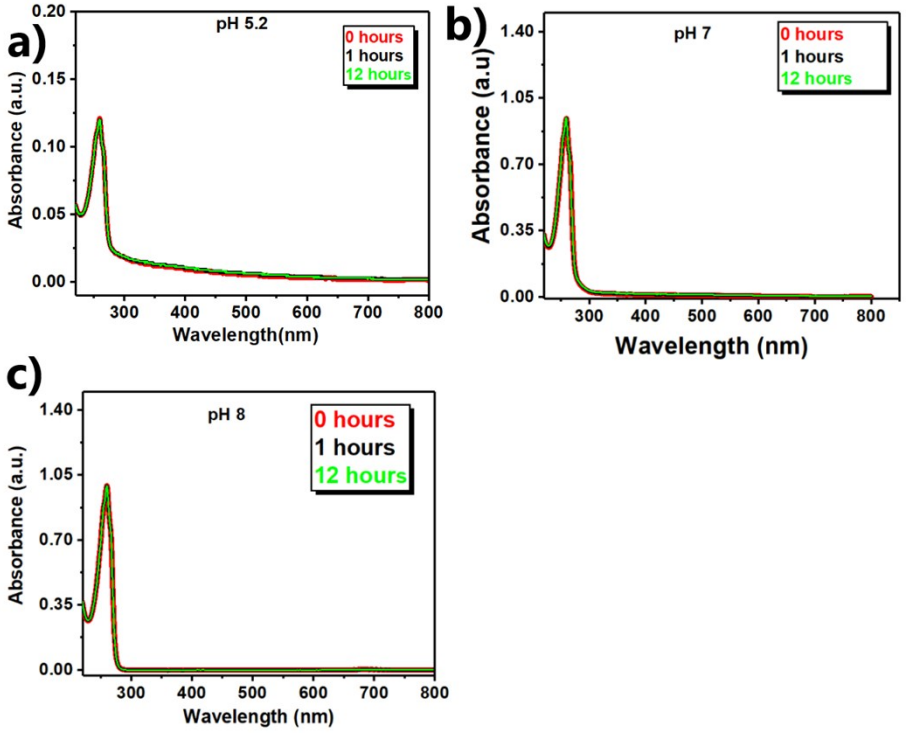

Figure S14: Comparative UV-Vis spectrum of Complex **1** recorded before (BEcWO) and after (AEcWO) the electrochemical water oxidation study i.e. Chronoamperometry stability.

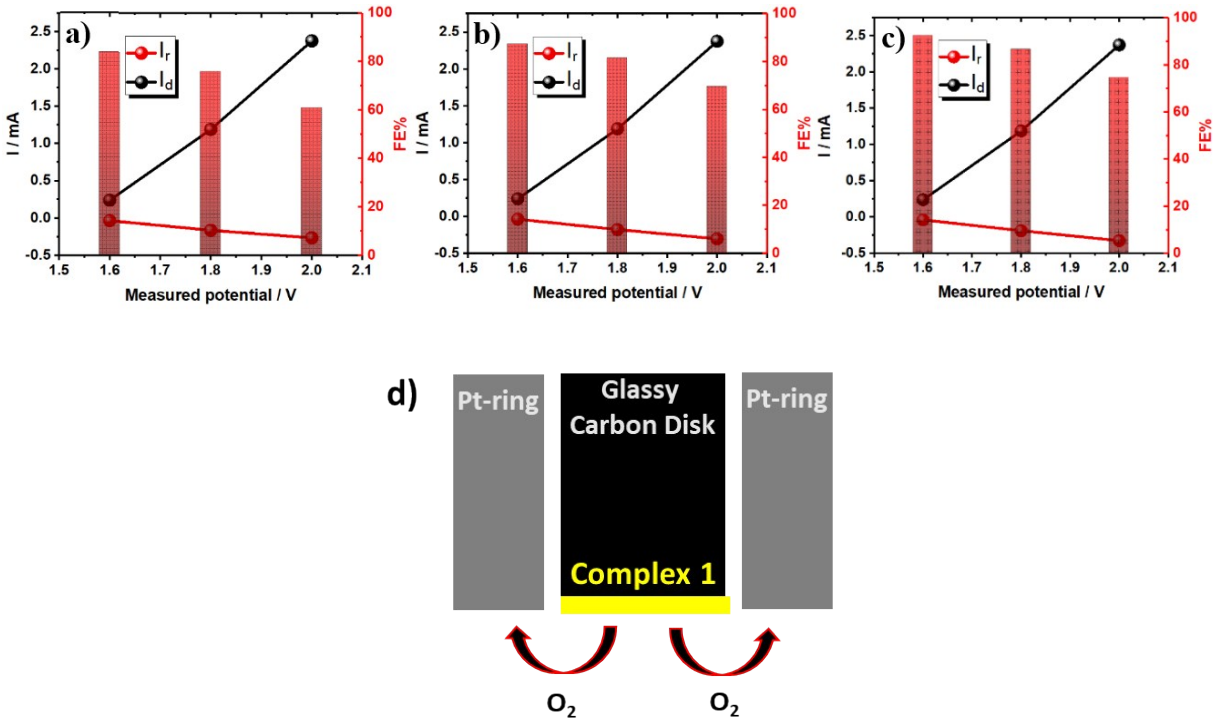

Figure S15: Faradaic efficiency of the catalyst at 1600 rpm under N_2 saturated phosphate buffer solution of different pH a) 5.2, b) 7, and c) 8. The applied disk current (1, 5, and 10 mA/cm^2) and oxygen reduction ring currents of RRDE plotted with respect to measured disk potential along with the calculated Faradaic efficiency. (d) Pictorial presentation of reduction of O_2-product on Pt-ring electrode.

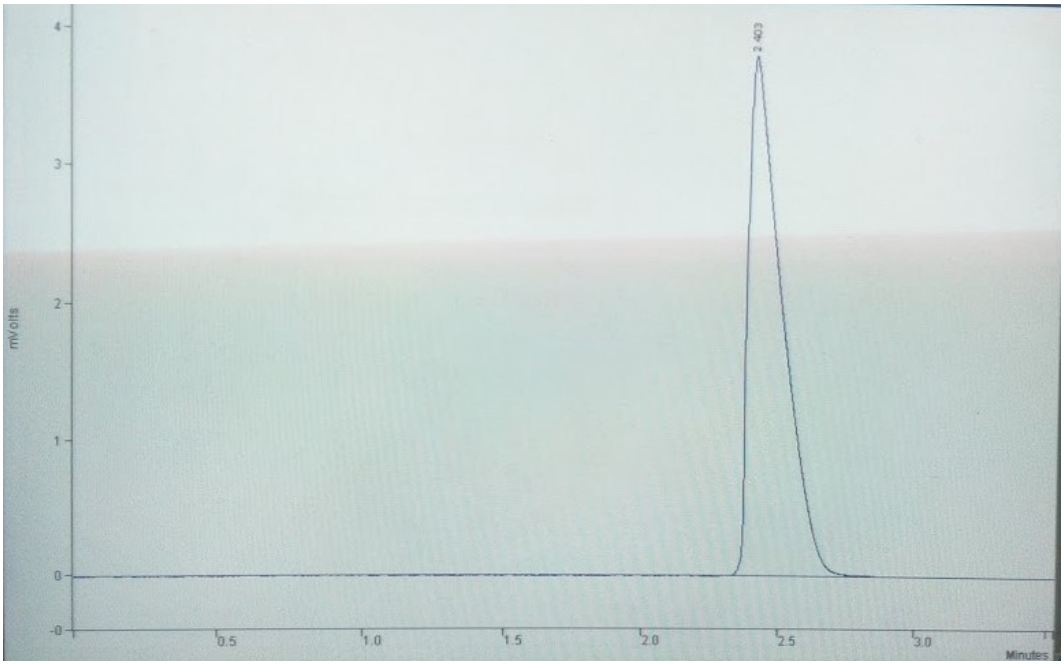

Figure S16a: Gas chromatogram BEcWO.

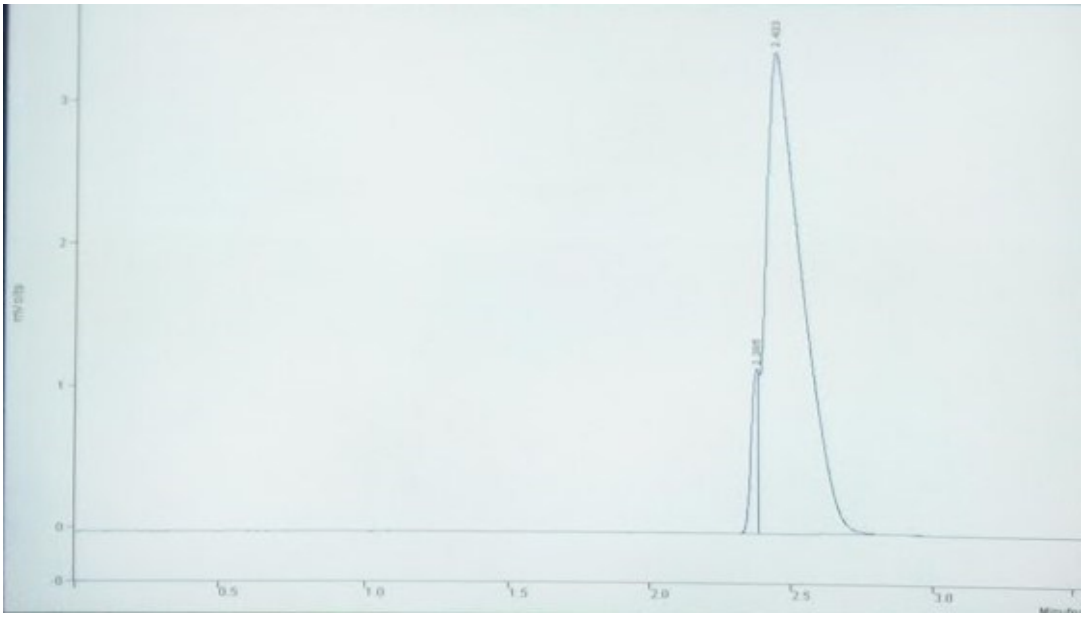

Figure S16b: Gas chromatogram while EcWO study.

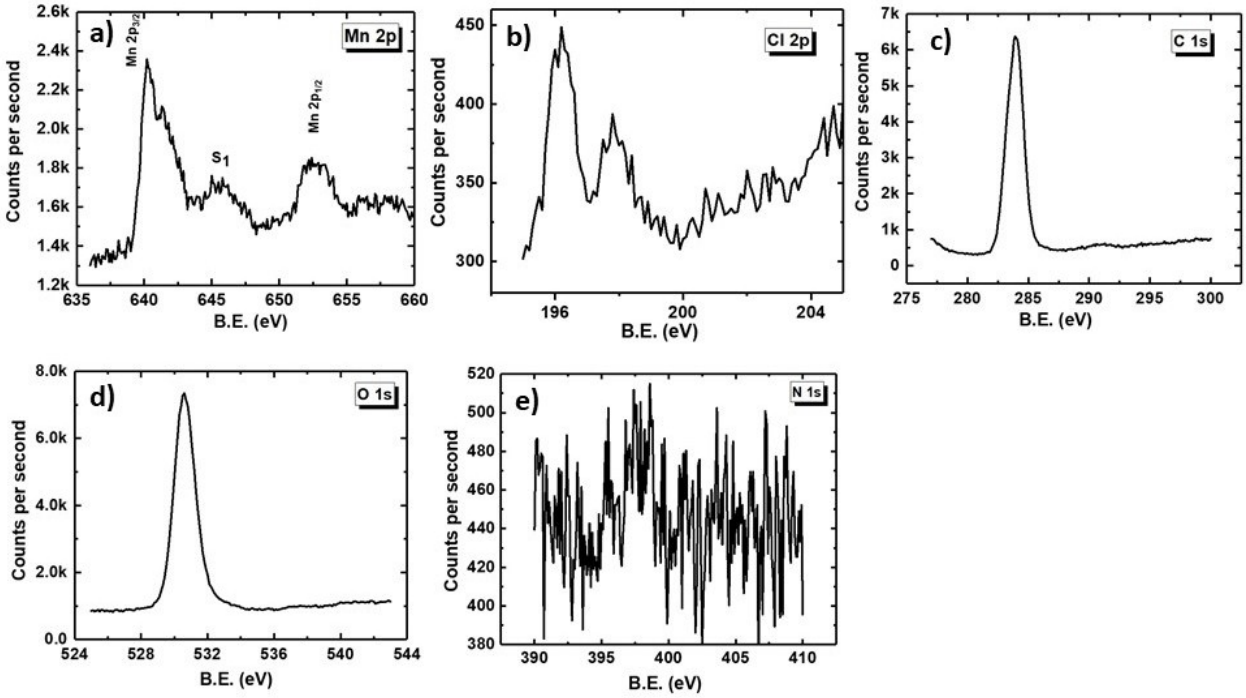

Figure S17: XPS of (a) Mn2p, (b) Cl2p, (c) C1s, (d) O1s, and (e) N1s of Complex **1** after electrochemical water oxidation (AEcWO).

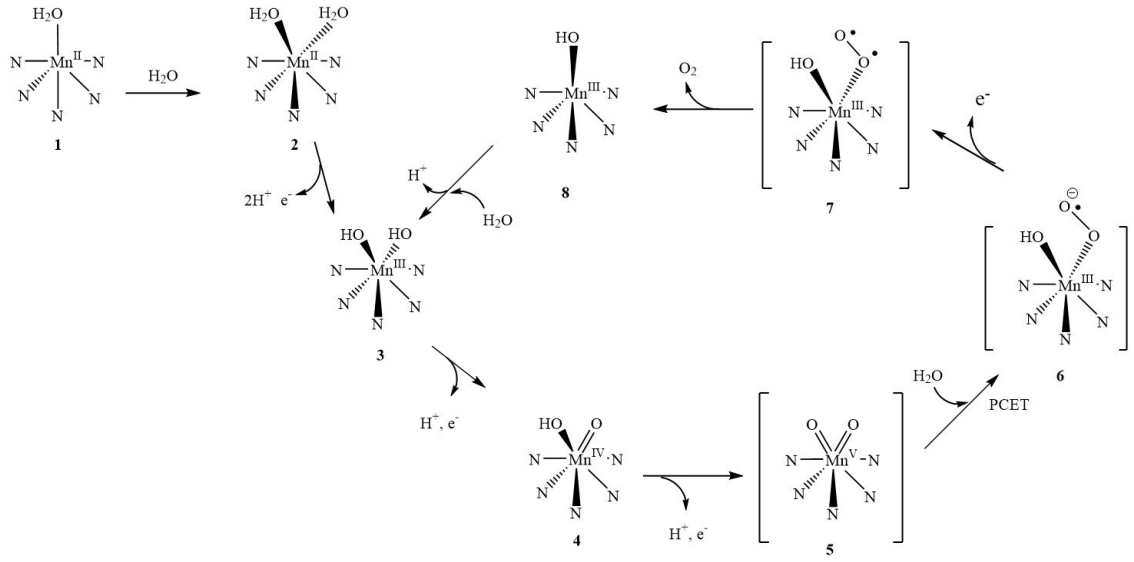

Figure S18: Proposed possible mechanism for electrochemical water oxidation by complex **1**.

Table S1: Technical details of data acquisition and selected refinement results for complex **1**.

Empirical formula	$C_{19}H_{31}Cl_2MnN_5O_9$
Formula weight	599.33
Crystal description	block
Crystal colour	white
Crystal system	Monoclinic
Space group	$P2_1/c$(no. 14)
Temperature (K)	100(2)
Unit cell dimensions	a = 8.983(3)Å
	b = 33.268(11)Å
	c = 8.791(3) Å
	α = 90.00°
	b = 105.287(4)°
	γ = 90.00°
volume (Å^3)	2534.4(15)
Z	4
Radiation type (Mo-Kα)/Å	0.71073
Crystal size (mm^3)	0.40 x 0.20 x 0.20
Diffractometer	Bruker APEX-II CCD
Absorption correction	Multi scan
No. measured reflections	9794
Calculated density (mg/m^3)	1.571
Absorption coefficient (mm^{-1})	0.790
F(000)	1247
θ range for data collection	2.35 to 24.99
Limiting indices	$-10 \leq h \leq 10$
	$-38 \leq k \leq 39$
	$-10 \leq l \leq 10$
Refinement method	Full-matrix least-squares on F^2
Data / restraints / parameter	4470 / 0 / 344
Final R Indices[I>2σ(I)]	R_1 = 0.0401, wR_2 = 0.0953
R indices (all data)	R_1 = 0.0440, wR_2 = 0.0977
Goodness of fit on F^2	1.042
Largest diff. peak and hole(eÅ^{-3})	1.0754 and -0.7223
Reflections collected / unique	30133 /4470 [R(int) = 0.0571]

Table S2: Selected bond lengths (Å) and angles (°) for complex **1**

Complex **1**			
Bond length (Å)			
Mn1—N3	2.257(4)	Mn1—N4	2.233(5)
Mn1—N5	2.330(2)	Mn1—N1	2.259(4)
Mn1—N2	2.333(3)	Mn1—O9	2.201(2)
Bond angle (°)			
N5—Mn1—N3	74.10(8)	N1—Mn1—N2	78.57(7)
N2—Mn1—N3	175.23(7)	N1—Mn1—N4	148.98(8)
N2—Mn1—N5	109.63(8)	O9—Mn1—N3	85.58(7)
N4—Mn1—N3	102.50(8)	O9—Mn1—N5	156.84(8)
N4—Mn1—N5	95.00(8)	O9—Mn1—N2	91.31(7)
N4—Mn1—N2	74.47(7)	O9—Mn1—N4	100.24(7)
N1—Mn1—N3	105.30(7)	O9—Mn1—N1	95.38(8)
N1—Mn1—N5	79.79(9)		

Note: The values in the parentheses indicate estimated standard deviations.

References:

[1] D. D. Narulkar, A. K. Srivastava, R. J. Butcher, K. M. Ansy, S. N. Dhuri, *Inorganica Chimica Acta.,* 2017, **467**, 405-414.

[2] https://xpssimplified.com/elements/manganese.php

[3] (a) J. P. McEvoy, G. W. Brudvig, *Chem. Rev.,* 2006, **106**, 4455–4483. (b) J. Barber, *Chem. Soc. Rev.,* 2009, **38**, 185–196. (c) C. S. Mullins and V. L. Pecoraro, Coord. *Chem. Rev.,* 2008, **252**, 416–443. (d) Y. Gao, T. Akermark, J. Liu, L. Sun, B. Akermark, *J. Am. Chem. Soc.,* 2009, **131**, 8726–8727. (e) Y. Shimazaki, T. Nagano, H. Takesue, B. H. Ye, F. Tani, Y. Naruta, *Angew. Chem., Int. Ed.,* 2004, **43**, 98–100.